JOURNAL OF AERONAUTICS AND SPACE TECHNOLOGIES
(ISSN : 1304-0448)
July 2021 Volume 14 Number 2
jast.hezarfen.msu.edu.tr

Research Article

Noise Reduction of Open Cavities by Passive Flow Control Methods at Transonic Speeds using OpenFOAM

Oğuzhan DEMİR[1*], Bayram ÇELİK[2], Kürşad Melih GÜLEREN[3]

[1] *Roketsan Missiles, 06780, Elmadag, Ankara, Turkey, oguzhan.demir.1@roketsan.com.tr,* https://orcid.org/0000-0002-8502-5295

[2] *Istanbul Technical University, Department of Astronautical Engineering, 34469 Sariyer, Istanbul, Turkey, celikbay@itu.edu.tr, https://orcid.org/0000-0002-7025-6330*

[3] *Eskisehir Technical University, Faculty of Aeronautics and Astronautics,, 26555 Tepebasi, Eskisehir, Turkey, kmguleren@eskisehir.edu.tr, https://orcid.org/0000-0003-3464-7956*

** Corresponding Author*

Article Info

Received: *March 02, 2021*
Accepted: *June 18, 2021*
Online: *July 26, 2021*

Keywords: Cavity Flow, Passive Flow Control, Transonic, OpenFOAM, Detached Eddy Simulation

Abstract

Flow over a cavity is one of the most intriguing problems in aeronautics. Although geometry is simple, the physics of cavity requires uttermost attention. In this study, various novel passive flow control techniques such as reshaping the aft wall as stair-stepped configuration or combinations of spoilers with reshaped aft wall are applied to cavity and effects of these techniques are investigated numerically. Combined configurations that are proposed in the present study are considered as a novelty to the literature. Analyses are performed with Detached Eddy Simulation method three-dimensionally in transonic regime (0.85 Mach) for a Reynolds number of ~10^7 based on the cavity length, 0.508 m, using open-source software OpenFOAM. Results are compared with both experimental data and each other, fundamentally in terms of Overall Average Sound Pressure Level. Further examinations are also performed for features such as Mach number, turbulent intensity and turbulent coherent structures. It is seen that combined passive flow control methods have reduced Overall Average Sound Pressure Level by ~10 dB. Newly proposed passive flow control methods have also reduced Overall Average Sound Pressure Level by ~6 dB. A high correlation between coherent turbulent structures and generated noise is observed.

To Cite This Article: O. Demir, B. Çelik, K. M. Güleren, "Noise Reduction of Open Cavities by Passive Flow Control Methods at Transonic Speeds using OpenFOAM", Journal of Aeronautics and Space Technologies, Vol. 14, No. 2, pp. 193-208, July. 2021.

Açık Kavitelerde Transonik Hızlarda OpenFOAM Kullanılarak Pasif Akış Kontrol Yöntemleri ile Gürültü Azaltımı

Makale Bilgisi

Geliş: *2 Mart 2021*
Kabul: *18 Haziran 2021*
Yayın: *26 Temmuz 2021*

Anahtar Kelimeler: Kavite Akışı, Pasif Akış Kontrolü, Transonik, OpenFOAM Ayrık Burgaç Benzetimi

Öz

Kavite akışları, havacılık alanındaki en ilgi çekici problemlerden birisidir. Bu çalışmada, kavite arka duvarını merdivenimsi bir yapıda yeniden şekillendirmek veya arka duvarı yeniden şekillendirilmiş bir kaviteye spoyler ekleyerek bileşik bir yöntem haline getirmek gibi birçok yenilikçi pasif akış kontrol tekniği uygulanmış ve bu yöntemler sayısal olarak detaylı bir şekilde incelenmiştir. Kavite arka duvarının yeniden şekillendirilip spoyler ile birlikte uygulandığı bileşik yöntemler özgün ve literature katkıda bulunabilme potansiyeline sahip olarak düşünülmektedir. Analizler Ayrık Burgaç Benzetimi yöntemi kullanılarak, üç boyutlu bir şekilde, transonik akış bölgesinde (0.85 Mach), kavite uzunluğu (0.508 m) temel alınarak ~10^7 Reynolds sayısında, açık kaynak kodlu mühendislik yazılımı OpenFOAM kullanılarak gerçekleştirilmiştir. Sonuçlar hem deneysel verilerle hem de kendi aralarında Ortalama Ses Basınç Tayf Düzeyi anlamında incelenmiştir. Ek olarak, Mach sayısı, türbülans yoğunluğu ve türbülanslı yapılar açısından da incelemeler yapılmıştır. Uygulanan yöntemlerle ~10 dB seviyelerinde gürültü azaltımı elde edilmiştir. Yenilikçi olarak önerilen yötenmlerde ise ~6 dB gürültü iyileştirmesi görülmüştür.

1. INTRODUCTION

Flow over cavity is one of the major research subjects in the fields of aerodynamics and aeroacoustics since 1950s when the concept of internal weapon bays was first shown up [1-2]. Over time, it has been investigated detailed both experimentally [3] and numerically [4]. Internal weapon bays are advantageous in terms of reducing the radar cross section and aerodynamic heating of a fighter. Over the years, enhancing technologies and new high-level requirements of the military operations which demand high speeds and low radar visibility have increased the interest in internal weapon bays. The flow over an internal weapon bay is termed as cavity flow.

Flow over cavities is generally divided into three categories based on the behavior of the generated shear layer caused by the cavity itself: open, transitional and closed cavities, respectively. Extensive studies conducted by Stallings and Wilcox [5] and Plentovich et al. [6] have aimed to define the boundaries of this categorization. Briefly, open cavities generally have a L/D ratio, L represents the length and D represents the depth of a cavity, of less than 10 whereas closed cavities generally have a L/D ratio of more than 13. Between these general boundaries, transitional cavity flows occur. Despite the L/D ratio has a substantial influence on the cavity type characterization, other parameters such as W/D ratio and flow regime do affect the flow type. Schematic representation of open and closed cavities for various flow regimes is shown in Figure 1. In open cavities, the shear layer has sufficient energy to bridge the cavity and reach the cavity aft wall without any impingement on the cavity floor. Since cavity flow is a time-dependent and highly unstable type of flow, the generated shear layer oscillates over the cavity and creates instabilities. After the separation of freestream flow from the cavity leading edge, these instability waves start to occur periodically. These instability waves form so-called Kelvin-Helmholtz vortices that are generated by Kelvin-Helmholtz instability. The main source of this vortex generation is the velocity difference between the freestream and the cavity zone. A schematic representation of open cavity flow is given in Figure 2.

The shedding of vortex occurs when the flow separates at the cavity leading edge and starts to spread downstream, eventually impinges on the aft wall of the cavity which is shown as impingement zone in Figure 2. The feedback mechanism that is given in Figure 2 occurs as a result of the shear layer formation. The impingement of the shear layer and vortices to the cavity aft wall generates a pressure wave which travels upstream that is indicated as the feedback. The impingement region, basically the aft wall, is therefore the main source of the generated pressure waves and acoustics. Generated acoustic waves interact with the oncoming shear layer at the impingement zone and excite the shear layer at resonant frequency which forces the flow in an acoustic manner, called acoustic forcing.

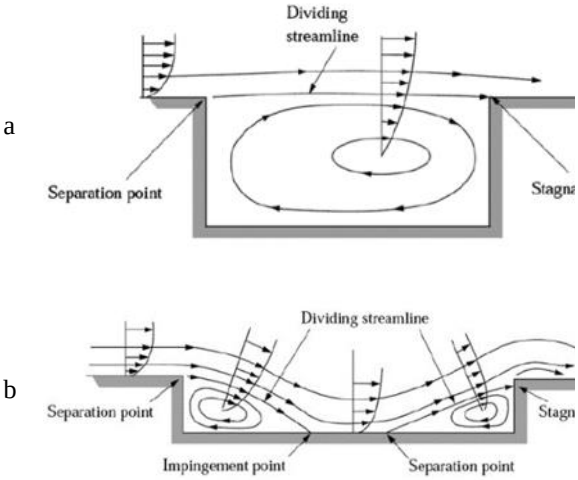

Figure 1. Schematic representations of a) open cavity b) closed cavity in subsonic regime [45].

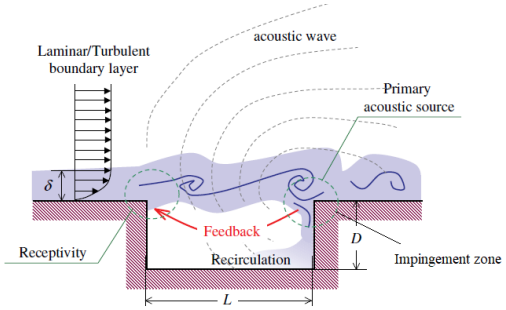

Figure 2. Schematic representation of cavity flow and feedback mechanism [7].

Due to highly unsteady and energetic flow field generated by cavity which causes vibrational and acoustic problems, analysis of these type of flows should be carried with attention. Such detailed analyses are now possible and affordable with the developing computing technologies over the last decades.

Due to acoustic scattering of turbulence at the aft edge of the cavity, high Sound Pressure Level (SPL), large pitching moments and pressure oscillations may have been seen in the cavity field and potentially may harm the structural integrity and prevent appropriate release of the store from the weapon bay or the complete flight system. First known studies that had an attempt to control the cavity flow were conducted by Norton [8] and Rossiter [9, 10]. Both Norton and Rossiter have suggested the use of spoilers ahead of the cavity for the aim of changing the Reynolds number of the boundary layer, suppressing the pressure oscillations and eventually decrease the noise level. Lamp [11] and Arunajatesan [12] have observed that the increasing the energy of shear layer is also an alternative to reduce the noise level. The smaller coherent vortex structures the flow has, the more reduction in noise generation.

Geometrical modifications of the cavity such as slanting the cavity walls (especially aft wall) or changing their shape, may also be useful in terms of noise and oscillation reduction. Smoothing the impingement of shear layer to cavity aft wall may create smaller oscillations in pressure and lower-magnitude acoustic waves [12, 13]. Passive flow control may be summarized as the geometrical modifications of the cavity or addition of external devices to the system such as spoilers, vortex generators, flaps, fences, resonance tubes and so on [10]. There are numerous studies that have been conducted over the years about passive flow controls such as usage of slanted wall, different kind of spoilers, rods, porous walls, vortex generators, wall dimples, and so on [13, 20-36, 44-46, 48, 49]. In open literature, there exist various studies focusing on the review of passive flow control methods [14, 15, 16, 19].

Internal weapon bays of the famous United States Air Force (USAF) fighter F-111 were investigated by Shaw et al. [17] using a 1/20.4 scaled model with different types of spoilers. As a result of this study, they have concluded that for open cavities, the broadband acoustic level was reduced; however, the impact on the high amplitude tones were insufficient for Mach 0.9. These inefficacies were suppressed when the freestream Mach number was increased to 1.2. The frequencies were also vanished for the case where freestream Mach number was 1.2. The same fighter model (F-111) was used by Smith et al. [18] to examine the effectiveness of a transverse rod spoiler rather than a flat spoiler. They have observed that both the location and diameter of the rod are important in the suppression of cavity noise.

Lawson and Barakos [13] have studied the effect of slanting the cavity aft wall since the major noise source of the cavity flow is the interaction of the shear layer with the aft wall. They have conducted numerical analyses of passive flow controls for spoilers, transverse rods and slanted walls. They have seen that all of the applied flow control methods have reduced the generated noise and eventually SPL. The lowest SPL was measured for the case where cavity aft wall was slanted. However, acoustic tones were still present with lower magnitudes. In recent years, an extensive effort has been put into the control of cavity flows. Saddington et al. [19] have examined numerous distinct passive flow control methods such as wall modifications, porous wall implementation, spoilers and sub-cavity fore of the main cavity. They have concluded that the spoiler usage is more efficient than the aft wall modifications and stated that with the usage of flat spoilers, Overall Average Sound Pressure Level (OASPL) reduction was achieved as ~8.8 dB. In another study where Gautam et al. [42] have investigated flow control using aft wall offset and cavity floor injection simultaneously, 31 dB reduction in OASPL was found for a cavity with L/D ratio of 3 in supersonic flow. Mancini et al. [44] have examined the M219 cavity numerically with several wall modifications. Deduction from this study was that the inclination of cavity aft wall by 45° was the most efficient passive flow control among those that were applied in the mentioned study.

In this study, additional to the studies that were aforementioned in previous paragraphs, various novel passive flow control techniques such as reshaping the cavity aft wall in a stair-stepped configuration or combinations of spoilers with reshaped cavity aft wall as a combined method are applied to cavity problem and effects of these techniques in the flow field are investigated numerically in detail. To the best of authors' knowledge, this is the first time that a flow control method that combines a spoiler configuration and aft wall modification has been studied. Besides, some of the aft wall modifications such as spline shaped aft wall and stair-stepped aft wall are believed to be applied for the first time in open literature within the research conducted by the authors. Combined configurations of aft wall reshaping and spoiler placement to fore of the cavity that are proposed and modeled in the present study are novel and have a potential to contribute to the literature. Analyses are performed three-dimensionally with Detached Eddy Simulation (DES) method in transonic regime (0.85 Mach) for a Reynolds number of ~10^7 based on the cavity length, 0.508 m, using open-source software OpenFOAM [35] with $k-\omega SSTDES$ modeling. As far as the authors are aware such an extensive numerical research using the $k-\omega SSTDES$ formulation of OpenFOAM for transonic cavity control is used for the first time in this study. Results are compared with both experimental data and each other, fundamentally in terms of OASPL. Additional examinations are also performed for other flow field parameters such as Mach number, turbulent intensity and turbulent coherent structures.

2. METHODOLOGY

2.1. Governing Equations

The governing equations of this turbulent, time dependent external aerodynamics problem are compressible Navier-Stokes equations [35] with DES implementation based on $k-\omega\ SST$ turbulence model. It is assumed that the perfect gas relations are valid and the flow is in thermodynamic equilibrium. The discretization of convective terms is done with a TVD scheme named 'Gauss limitedCubicV' to avoid undershoots and overshoots in the solution. GAMG methodology is followed for the linear solution of the pressure with DILU smoother. For other quantities such as velocity and turbulence, PBiCGStab solver with DILU smoother is applied. Lastly, the solver that is used in this computational study is rhoPimpleFoam which is a pressure-based solver for compressible turbulent flows. Thus, PIMPLE algorithm is used in the solution methodology.

2.2. Turbulence Modeling

The main idea of DES is to use RANS for near-wall treatments and LES for outside of the wall. The DES modification of the well-known RANS turbulence model implemented in OpenFOAM is used in this study [36]. In $k-\omega\ SSTDES$ model, transport equations for turbulent kinetic energy and specific turbulence dissipation rate are given in equations 1 and 2.

$$\frac{\partial(\rho k)}{\partial t}+\frac{\partial(\rho k U_i)}{\partial x_i}=\tilde{P}_k-\beta^* k\omega F_{DES}+\frac{\partial}{\partial x_i}\left[(\mu+\mu_t\sigma_k)\frac{\partial k}{\partial x_i}\right] \quad (1)$$

$$\frac{\partial(\rho\omega)}{\partial t}+\frac{\partial(\rho\omega U_i)}{\partial x_i}=\alpha\rho S^2-\rho\beta\omega^2+\frac{\partial}{\partial x_i}\left[(\mu+\mu_t\sigma_\omega)\frac{\partial\omega}{\partial x_i}\right]-2(1-F_1)\sigma_{\omega2}\frac{1}{\omega}\frac{\partial k}{\partial x_i}\frac{\partial\omega}{\partial x_i} \quad (2)$$

here $S=\sqrt{2S_{ij}S_{ij}}$ is the invariant measure of the strain rate. Strain rate tensor of the velocity can be computed as follows by equation 3:

$$s_{ij}=\frac{1}{2}\left(\frac{\partial U_i}{\partial x_j}+\frac{\partial U_j}{\partial x_i}\right) \quad (3)$$

The first blending function F_1 can be computed as shown in equation 4 [36].

$$F_1=tanh(\eta^4),\quad \eta=min\left[max\left(\frac{\sqrt{k}}{\beta^*\omega y},\frac{500\nu}{y^2\omega}\right),\frac{4\sigma_{\omega2}k}{CD_{k\omega}y^2}\right] \quad (4)$$

where y is the nearest distance to wall.

$CD_{k\omega}$ term in η formulation is defined as in equation 5,

$$CD_{k\omega}=max\left(2\rho\sigma_{\omega2}\frac{1}{\omega}\frac{\partial k}{\partial x_i}\frac{\partial\omega}{\partial x_i},10^{-10}\right) \quad (5)$$

The turbulent eddy viscosity is defined by equation 6:

$$\nu_t=\frac{\mu_t}{\rho}=\frac{a_1 k}{max(a_1\omega,SF_2)} \quad (6)$$

where a_1 is the square root of β^*. F_2 is the second blending function which is formulated as in equation 7,

$$F_2=tanh(\zeta^2),\quad \zeta=max\left(\frac{2\sqrt{k}}{\beta^*\omega y},\frac{500\nu}{y^2\omega}\right) \quad (7)$$

where y is the wall distance.

A limiter of turbulent kinetic energy production exists on the SST model in order to prevent the build-up of turbulence in stagnation regions. The limiter is defined as shown by equations 8 and 9:

$$\tilde{P}_k=min(P_k,10\cdot\beta^*\rho k\omega) \quad (8)$$

$$P_k=\mu_t\left(\frac{\partial U_i}{\partial x_j}+\frac{\partial U_j}{\partial x_i}\right)\frac{\partial U_i}{\partial x_j} \quad (9)$$

In the DES formulation of this turbulence model, the function F_{DES} is implemented in the dissipation term of turbulent kinetic energy transport equation via equation 10:

$$F_{DES}=max\left(\frac{L_t}{C_{DES}\Delta},1\right) \quad (10)$$

where L_t is the turbulent length scale and calculated as $L_t=\sqrt{k}/(\beta^*\omega)$; Δ is the maximum local grid spacing which is defined as $\Delta=\max(\Delta x,\Delta y,\Delta z)$ and C_{DES} is a calibration constant with the value of 0.61.

In the case of a sufficiently fine grid, the term F_{DES} goes beyond the value of 1 which will in turn reduce turbulent kinetic energy and viscosity and make the problem unsteady. Therefore, when the local grid is sufficiently fine so that the turbulence can be resolved, DES model will decrease the amount of modeled turbulent shear stress and will switch to LES methodology for that region. The value of blending function F_1 varies between 1 and 0; in regions close to wall, the value is 1 and the model switches to $k-\omega$, whereas in regions outside of the boundary layer the value becomes 0 and the model switches to $k-\epsilon$. Additional to blending function, constants that are placed in the formulation are also blended. The blending of model constants are done as presented in equation 11.

$$\chi=F_1\chi_1+(1-F_1)\chi_2 \quad (11)$$

where χ is a general notation for β and α parameters. Another way of blending the model constants is given in equation 12:

$$\frac{1}{\psi}=F_1\frac{1}{\psi_1}+(1-F_1)\frac{1}{\psi_2} \quad (12)$$

where ψ is a general notation for σ_{kj} and σ_{wj} constants. Values of model constants are given in Table 1. [36]:

Table 1. Model constants of SST turbulence model.

Model constant	Value
α_1	5/9
α_2	0.44
β_1	3/40
β_2	0.0828
$1/\sigma k_1$	0.85
$1/\sigma k_2$	1
$1/\sigma_{\omega1}$	0.5
$1/\sigma_{\omega1}$	0.856

Further details of turbulence modeling can be found in [36].

2.3. OASPL Calculation

OASPL is the logarithmic addition of all the discrete spectral sound pressure levels (SPL) into a single figure. In this study, noise generated by the cavity is calculated in terms of OASPL, as shown in equation 13.

$$OASPL\ (dB)=20\log_{10}\left(\frac{p_{rms}}{p_{ref}}\right) \quad (13)$$

where p_{rms} is the root mean square (RMS) of pressure. The standard for the minimum perceivable sound p_{ref} has the value of $2\text{x}10^{-5}$ Pa. The RMS of pressure may be defined as

$$p_{rms}=\frac{1}{N}\sum_{i=1}^{N}\frac{(p_i-p_{mean})^2}{N} \quad (14)$$

In equation 14, N indicates the number of pressure data gathered, p_{mean} indicates the mean value of pressure

throughout the measurement and p_i indicates the instantaneous value of pressure. Mean value of pressure can be calculated as in equation 15.

$$p_{mean} = \frac{1}{N}\sum_{i=1}^{N} p_i \quad (15)$$

Fast Fourier Transform (FFT) is also applied to the gathered pressure data for the aim of obtaining Power Spectral Density (PSD). PSD indicates the RMS of pressure versus frequency and gives an insight about the frequency content within the overall spectrum. Discrete acoustic tones, so called Rossiter modes, can be seen by inspecting the PSD graphs. In this study, PSD investigations of baseline cavity geometry are performed in order to ensure the validity of the numerical setup.

2.4. Problem Statement

M219 cavity configuration which has an orthogonal cavity cross-section is a well-known case in cavity investigations and taken as reference in numerous studies [13, 19, 31, 39, 40]. Experimental study by Nightingale et al. [46] is taken as the reference experiment in the present study. Details regarding to M219 cavity case problem are given in Table 2.

Table 2. Cavity dimensions and Mach number for the study of Nightingale et al. [46].

L (m)	D(m)	W (m)	L/D	W/D	Freestream Mach Number
0.508	0.1016	0.508	5	5	0.85

The numerical study that is taken as the reference is the study of Larcheveque et al. [16]. In their study, they have conducted numerous LES simulations for the three dimensional M219 cavity for a Reynolds number of $7x10^6$. Extensive comparisons with the available experimental and numerical data are made and a satisfactory level of accuracy was achieved.

2.5. Proposed Configurations for Noise Reduction

M219 clean cavity where no passive/active control method is of the case, is the baseline problem of the present study. Various innovative and novel passive flow control methods in order to suppress the pressure oscillations and to reduce the OASPL generation are applied. Applied flow control methods are tabulated in Table 3. The problem statement of the present study is as follows:

- Understanding the physics of the cavity flow and making an effort to improve the flow environment when a cavity is present.
- Investigating the unsteady behavior of three-dimensional cavities where the flow is compressible, transonic (0.85 Mach) and turbulent.
- Suppressing the pressure oscillations encountered in cavity flows.
- Reducing the noise generated by cavities.

In order to achieve the desired goals, M219 clean cavity configuration (M219CC) is first taken into consideration and analyzed as the baseline geometry. Thereafter, intriguing various passive flow control methods are configured and applied to the baseline geometry such as stair-shaping the cavity aft wall or designing the cavity aft wall as a spline. These methods are believed to have an efficient noise reduction while being inventive. Additional to these methods, combined configurations of aft wall reshaping and spoiler placement to aft of the cavity are applied in the present study, which are also considered to be other novel attempts to reduce noise and suppress pressure oscillations. The original L/D ratio of 5 and W/D ratio of 1 are kept constant throughout the applied configurations as well as the freestream flow conditions. A complete brief description of applied passive flow control methods along with the aforementioned cases are given in Table 3.

Table 3. Proposed passive flow controlled cavity cases throughout the present study.

Configuration	Notation	Brief Description
M219 Clean Cavity	M219CC	Clean cavity configuration with no flow control
Aft Wall Configurations	PAW1	45° inclination of aft wall
	PAW2	45° semi-inclination of aft wall
	PAW3	Stair-shaped aft wall
	PAW4	Spline-shaped aft wall
Spoiler Configurations	PSP1	Rectangular bar shaped spoiler at front edge of cavity
	PSP2	Rectangular bar shaped spoiler at 0.1L upstream of cavity
Combined Configurations	PC1	Combination of PAW1 and PSP1
	PC2	Combination of PAW1 and PSP2

2.6. Computational Details

The numerical domain of the present study consists of upstream, side-stream and downstream walls along with the cavity region, as shown schematically in Figure 3. Additional slip boundaries are put to numerical domain to ensure that the mis-evolution and

alteration of flow caused by numerical boundaries is negligible. Shaded region in Figure 3 indicates the cavity region. For the grid generation, an in-house grid generator has been used. A structured grid which consists of hexahedral elements are generated for each case by following the log-law of the wall [39]. The dimensionless wall distance parameter y^+ is calculated prior to analyses and kept within the limits of log-law layer as 300 for upstream wall of the cavity for all computations. Additional y^+ independence studies are also conducted prior to the analyses of passive flow control techniques. Several reasons lie behind the decision of the value of y^+ being in log-law layer, such as the implementation of wall functions, large-scale coherent structures governed cavity flow physics [40, 42] and the need of reducing the total number of cells due to the limited available amount of CPUs. Proper wall functions are used for each cases in order to model the flow near the wall.

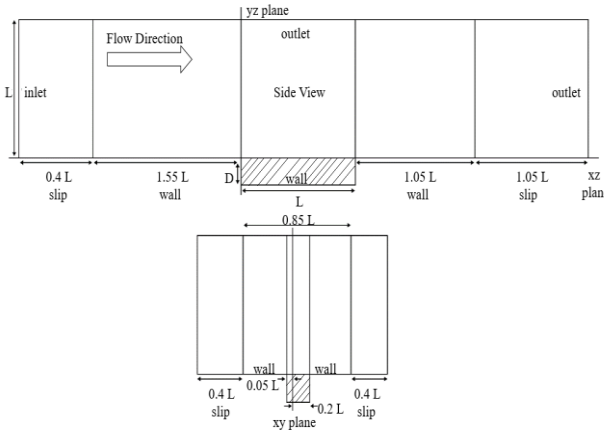

Figure 3. Schematic representation of the numerical domain, L=0.508 m.

Generated grid of the problem for clean cavity configuration is shown in Figure 4. As mentioned before, a grid convergence analysis is conducted by taking M219CC as the base case with different grid densities and different dimensionless wall distance parameter y^+ values. Details of the grid convergence study is given in Table 4. The ratio of cells within the cavity region to overall is kept constant around 10% for each study. The coarsest grid has 1.3 million cells whilst the finest grid has approximately 10.5 million cells. Cavity close-up side view of domain with arrows the edges of the cavity where the coarsening or refinement is performed for grid convergence study is shown in Figure 5. Additional to the edge refinements, inner region of cavity is also refined by increasing the grid points. The distribution of OASPL on cavity floor is taken as the point of interest in this grid independence study. Following to that, close-up side views of grids generated for passive flow control methods are presented in Figure 6.

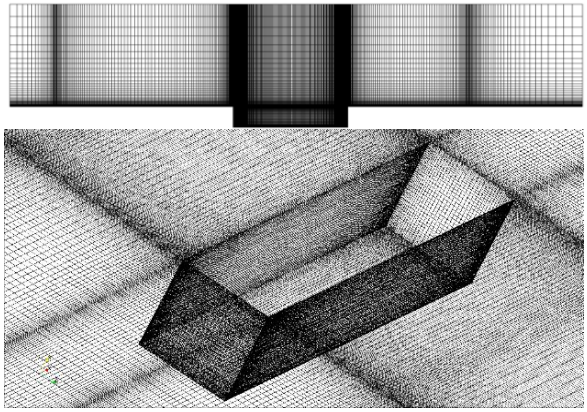

Figure 4. Structured grid of the M219CC domain, side view (top) and close-up cavity region view (bottom).

Table 4. Grid independence study details.

Case Name	Overall Cell Count	Cells in Cavity Zone	First Layer Thickness (m)	y^+ on upstream wall
Coarse (C1)	1.323 M	0.135 M	8.83×10^{-4}	300
Medium 1 (M1)	3.136 M	0.320 M	8.83×10^{-4}	300
Medium 2 (M2)	3.136 M	0.320 M	2.94×10^{-4}	100
Medium 3 (M3)	3.136 M	0.320 M	8.83×10^{-5}	30
Fine (F1)	6.125 M	0.625 M	8.83×10^{-4}	300
Very Fine (VF1)	10.8M	1.08M	8.83×10^{-4}	300

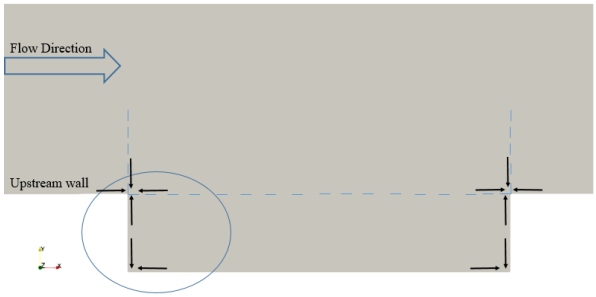

Figure 5. Grid refinement regions for grid convergence study.

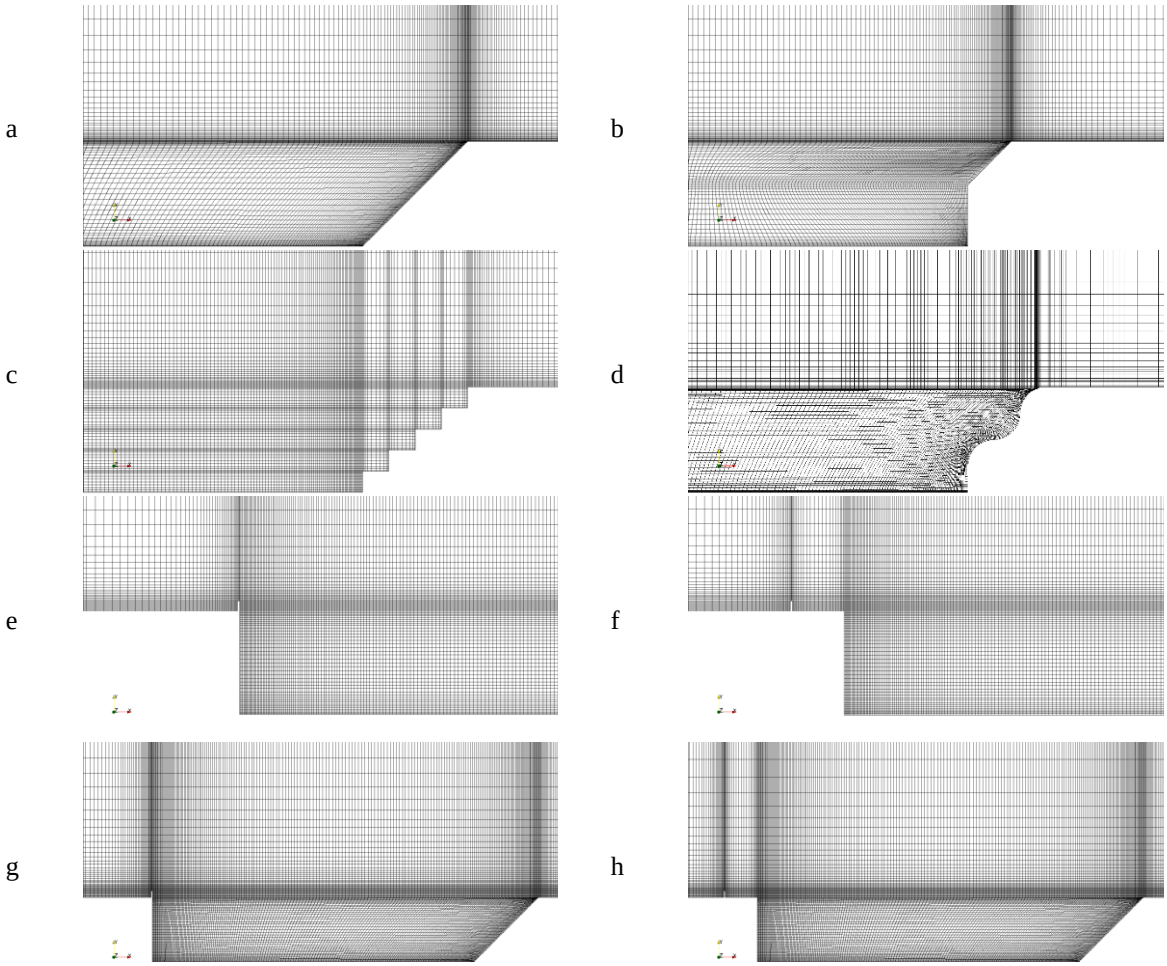

Figure 6. Close-up side view of cavity grid for passive flow control methods: a) PAW1 b) PAW2 c) PAW3 d) PAW4 e) PSP1 f) PSP2 g) PC1 h) PC2.

2.7. Solution Methodology

The present study is conducted using the open-source software OpenFOAM. The inlet has a Dirichlet type boundary condition whereas the outlet has a Neumann type boundary condition. Special attention is given to the outer boundaries of the problem to avoid the numerical reflection. For that reason, non-reflecting boundary condition of OpenFOAM is applied to inlet and outlet boundaries. The walls are specified as adiabatic walls and additional regions which are named as 'slip' are given with the symmetry boundary condition. Appropriate wall functions are used for wall boundaries. Analyses are conducted at sea level conditions. Freestream values of the flow at sea level are given in Table 5. It should be noted that only the analysis baseline case (M219CC) is conducted with the settings given in Table 5. Simulations of passive flow control methods are initialized with the last time step data of the M219CC. Simulations are run for 50 Convective Time Scales (CTS) where 1 CTS corresponds to the one passage of a flow particle through the cavity length L. Considering the current problem setup, 1 CTS corresponds to 1.76×10^{-3} seconds. In terms of the most dominant Rossiter mode (2^{nd} mode), 1 CTS may also be stated as 1.5 times the 2^{nd} Rossiter mode frequency. The time step is determined as 1/1500 of the 2^{nd} Rossiter mode frequency magnitude. Data of last 40 CTS are taken into consideration for post-processing the average flow field parameters. The flow field data of each 0.1 CTS are written and saved in time directories. Maximum CFL number is kept as 1 since a DES is performed in a turbulent compressible region. The residuals are both stored and plotted using the relevant function and flow variable Mach number, additional to the main variables is computed for each time step. Pressure data at each probe is stored for each 0.001 CTS. In order to perform OASPL calculations, RMS values of pressure are also computed at each time step. 1 CTS is calculated as:

$$1\ CTS = L/U_{\infty} \tag{16}$$

Table 5. Sea level freestream values of the flow.

Property	Value
Velocity (m/s)	289.325
Mach	0.85
Pressure (Pa)	101325
Temperature (K)	288.15
Reynolds number	1×10^{7}
Turbulence kinetic energy (m^2/s^2)	12.56
Specific dissipation rate (1/s)	8.56×10^{4}

3. RESULTS

3.1. Grid Convergence Study

Validation of the model is conducted prior to passive flow control method investigations. Grid convergence analysis is conducted by examining spectral behavior of the flow, OASPL distribution along cavity floor and mean flow field contours. Both grid resolution and y^+ effects are investigated. PSD measurements are compared with experimental and theoretical findings and it is seen that the discrete acoustic tones seen in open cavities (Rossiter modes) are captured well for each case which can be inspected via Figure 7. The first three dominant modes of Rossiter are captured prominently for each grid whereas the fourth mode was unclear due to the low magnitude of the peak.

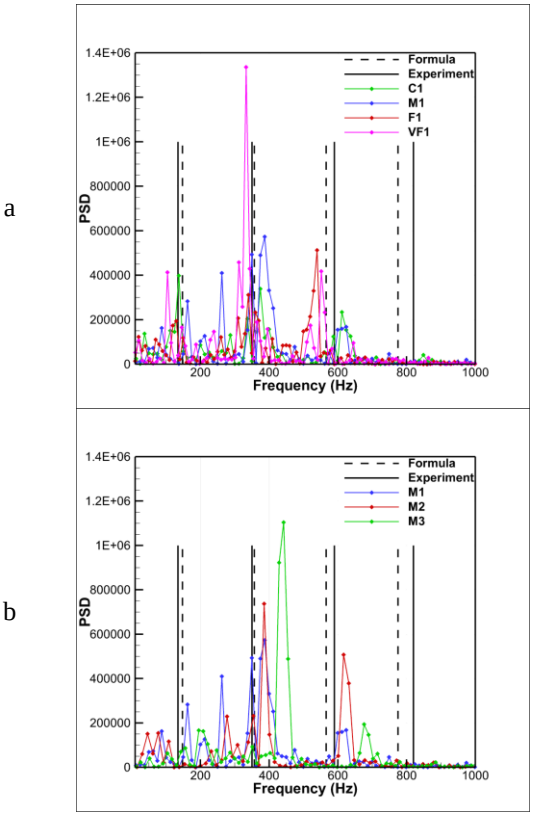

Figure 7. Spectral analysis (at x/L=0.95) on cavity floor for grid convergence study for M219CC with Rossiter's acoustic tones. a) Comparison for different grid numbers b) Comparison for different y^+ values.

Normalized longitudinal velocity profiles on central xy plane are also compared with the data of reference numerical study. Results of the longitudinal velocity profile are shown in Figure 8. The parameter that is shown as "s/D" represents the dimensionless distance in terms of cavity depth (D). It is observed that among six different grids, M1 case suits best with the reference data. Considering the results of velocity profile and acoustic tone investigation, M1 case is chosen for further simulations. Lastly, OASPL distribution on cavity floor at the mid-section of cavity for each case is compared. The main reason behind the selection of the mid-plane cross-section for OASPL distributions is that the most representative basic presentation of noise for this type of cavity is known to be that section. The results in Figure 9 show that an overprediction for all cases is present. M1 case is found to suit better to the experimental trend of OASPL distribution better than other cases. This overprediction is oftenly encountered when using URANS or hybrid RANS/LES methods such as DES and is believed to occur because of the numerical diffusion and artificial turbulence production [14, 31]. As a conclusion, grid independence study is performed and it is found that the y^+ variation is not crucial for cavity investigation as long as the log-law of the wall is followed. According to the gathered results, usage of wall functions is sufficient for spectral analyses for this problem. At this point, further studies that consist of detailed clean cavity analyses and passive flow control methods are performed using M1 grid.

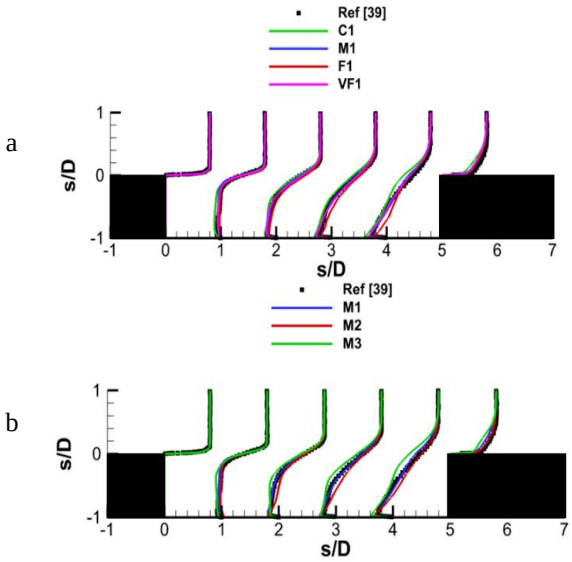

Figure 8. Mean longitudinal velocity profile for grid convergence study: a) Comparison of different grid resolutions b) Comparison of different y^+ resolutions.

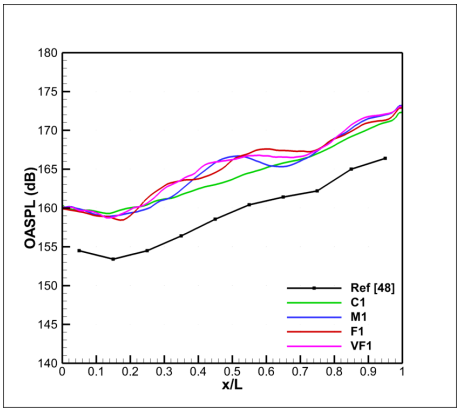

b

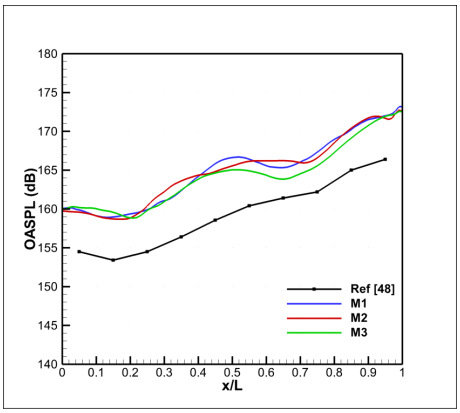

Figure 9. OASPL distribution at the mid-section of the cavity floor for grid convergence study a) For different cell numbers b) For different y^+ values.

3.2. Clean Cavity

Instantaneous flow contours of clean cavity are inspected in order to visualize the feedback mechanism and complex unsteady flow behavior. Figure 10 shows the evolution of a main stream-wise vortex within the cavity as an expected result of feedback mechanism. The snaps are taken at the mid-plane section of the cavity. The contours are taken at equally divided instantaneous time of the 2nd Rossiter mode period which is represented as t_{R2}, which is represented in Figure 7. It is also noticed that the flow is highly unsteady which has several vortices at different locations of the cavity. It is also a fact that since DES technique is applied, the instantaneous flow has a highly rotational behavior where both small and large vortices and recirculation areas are present.

Isosurfaces of Q-criterion for clean cavity configuration are represented in Figure 11. The result shows that the flow within the cavity is governed by large-scale coherent structures which are formed by the separation of shear layer from cavity leading edge and these structures densify near the cavity aft wall where the interaction of shear layer with the cavity aft wall occurs.

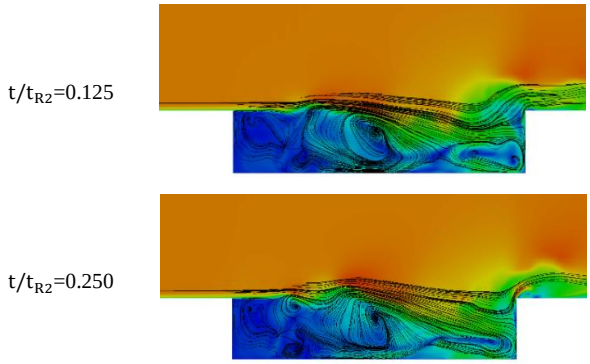

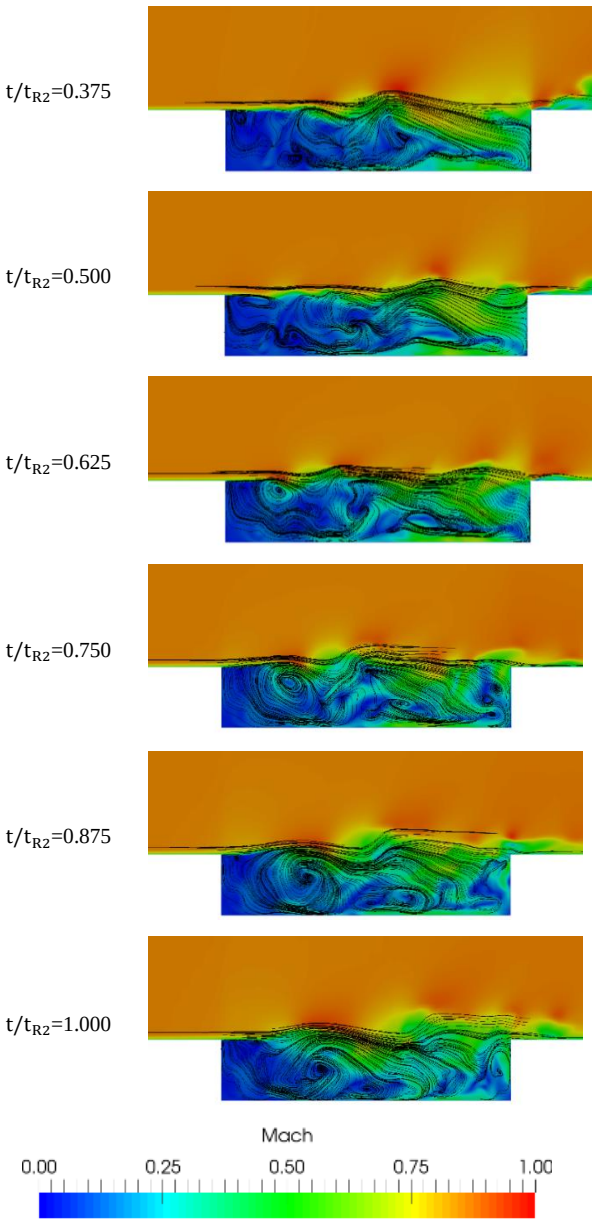

Figure 10. Instantaneous Mach contours of M219CC for one period of 2nd Rossiter mode.

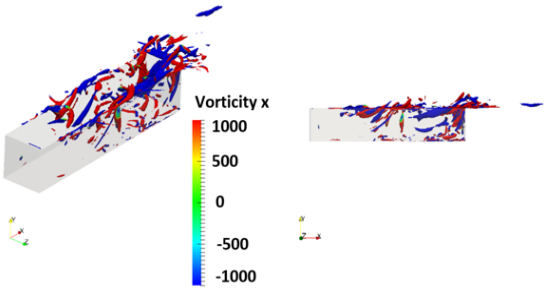

Figure 11. Isosurfaces of Q-criterion for clean cavity configuration colored by x-vorticity, t=50CTS (0.088 s).

3.3. Aft Wall Configurations

Mean flow contour results of cavity aft wall configurations are presented in Figure 12. It is observed that the general behavior of the shear layer shows almost no change whereas the turbulence intensity inside the cavity decreases slightly when an aft wall passive flow control method is applied. This alleviation is thought to be arise from the smoother collision of the shear layer with the aft wall. The highest reduction in turbulence intensity is seen in PAW1 configuration where the aft wall was inclined by 45°. As for the OASPL, all aft wall configurations reduced the OASPL distribution especially near the cavity front side. OASPL intensity at cavity aft wall is higher for PAW3 and PAW4 configurations compared to PAW1 and PAW2. Expansion of high OASPL values to out of the cavity was lowered when a passive flow control was applied. The difference in the acoustic propagation is seen obviously for each aft wall control technique. Figure 13 represents the OASPL distribution along the cavity floor at the mid-plane for aft wall configurations**.** Aft wall configurations have proven to be effective in terms of OASPL reduction. Since the main source of the noise generation is aft wall, changing the geometry of aft wall has decreased OASPL. PAW1 configuration is the best of applied configurations in terms of OASPL reduction. Reduction was measured as ~10 dB at the front half of the cavity floor. All configurations have given similar OASPL results near the cavity aft wall.

Isosurfaces of Q-criterion for aft wall configurations colored by x-vorticity are shown in Figure 14. It can be seen that less and smaller structures exist for aft wall configurations compared to M219CC. Chaotic structures present in front half of M219CC are no longer present for PAW1, PAW2 and PAW4. It is also noticed that the flow tends to be more rotational in aft wall configurations, especially in PAW3, than M219CC.

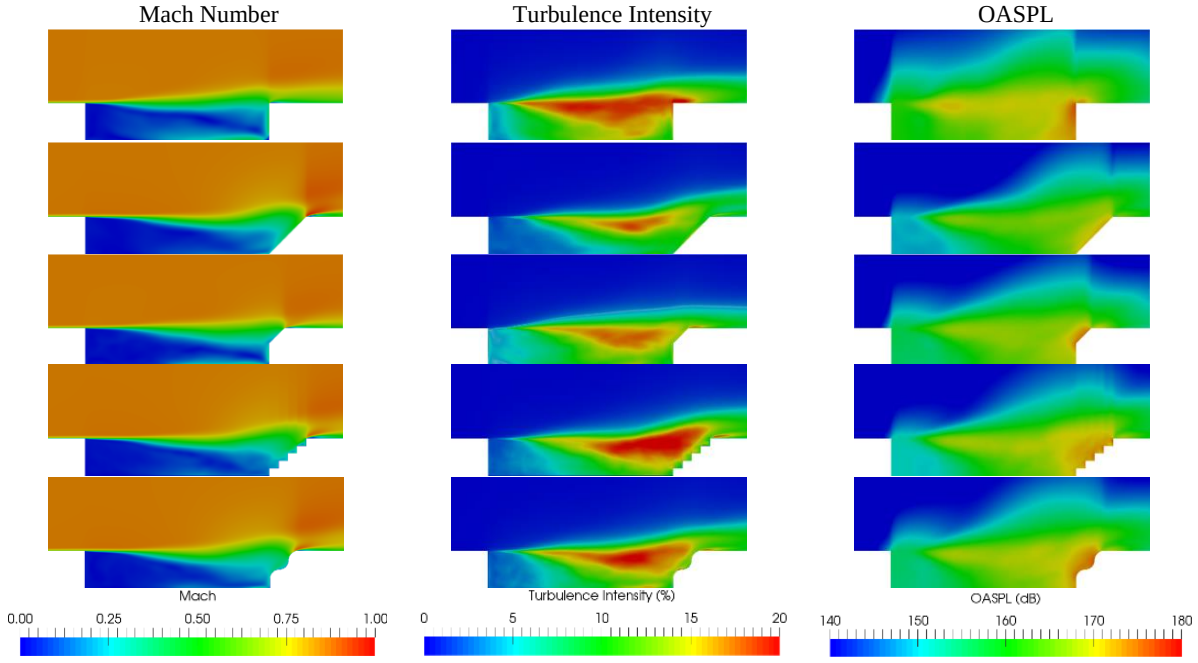

Figure 12. Mean Mach, turbulence intensity and OASPL (dB) contours for aft wall configurations (close-up, side view of the cavity region) a) M219CC b) PAW1 c) PAW2 d) PAW3 e) PAW4.

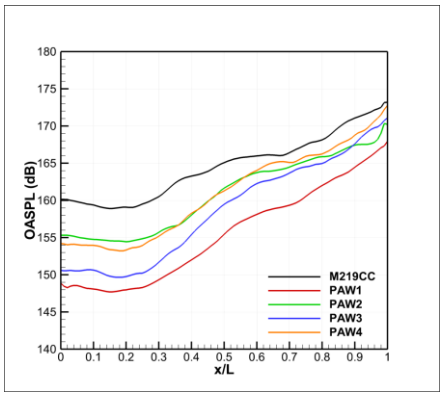

Figure 13. OASPL distribution at the mid-section of the cavity floor for different aft-wall modifications.

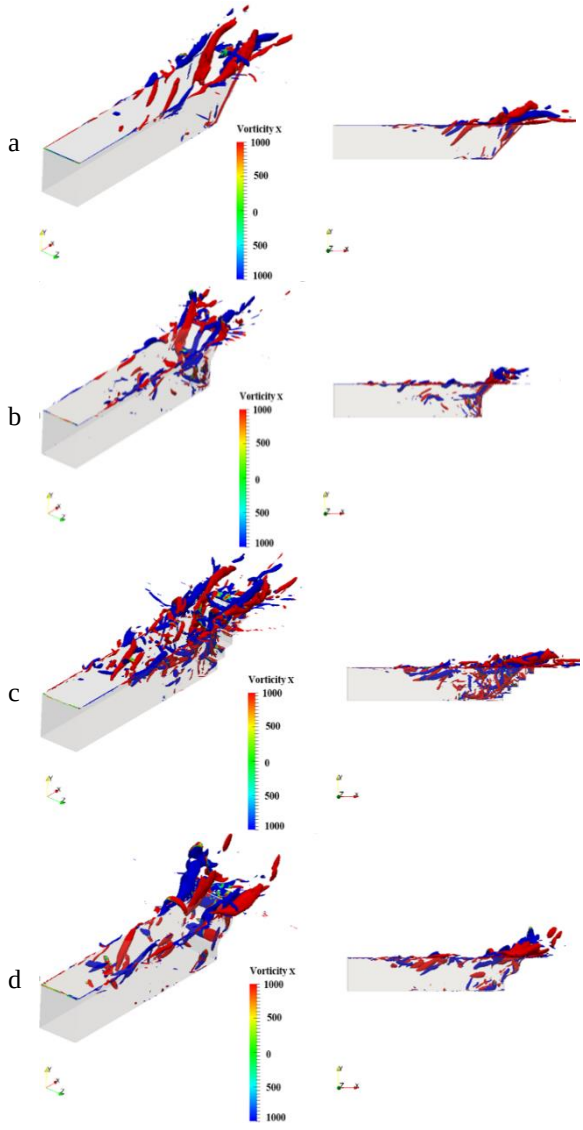

Figure 14. Isosurfaces of Q-criterion colored by Mach number for aft wall configurations a) PAW1 b) PAW2 c)PAW3 d) PAW4, t= 50 CTS (0.088 s).

3.4. Spoiler Configurations

Effects of spoilers located in two different positions upstream of the cavity are investigated in Figure 15. It can be seen from Mach contours that the spoilers have lifted the shear layer along the cavity mouth. Turbulence intensity inside the cavity is smaller for each spoiler configuration than M219CC since the shear layer is lifted up. As for the OASPL reduction, spoiler configurations have proven to be effective. OASPL has smaller values all along the cavity floor for each case.

Figure 16 shows the OASPL distribution at the mid-plane of the cavity floor for spoiler configurations. The trend of PSP1 and PSP2 are similar to that of M219CC whereas both configurations have reduced the OASPL. Isosurfaces of Q-criterion colored by x-vorticity given in Figure 17 represent the small structures caused by the placement of a flat spoiler upstream of the cavity. A similarity on isosurfaces of Q for PSP1 and PSP2 can be observed even though the location of spoiler was different on each configuration. More structures are present compared to M219CC near cavity aft region but they are smaller in size. Structures that exist about the mid-region of the cavity for M219CC do not exist on these cases. At each configuration, existence of spoiler has created a stagnation region at the impact location of flow to the spoiler, which can be seen as the green colored area at the frond edge of the spoiler in Figure 17. On both sides of this area, the flow has become rotational and a scattered to contrarious directions.

3.5. Combined Configurations

Combined configurations are tested as the last part of passive flow control methods, to examine the effect of two different control methods when applied simultaneously. Mean flow contours for M219CC, PAW1, PSP1, PSP3, PC1 and PC2 are presented in Figure 18. Similar to other shown passive flow control techniques, combined configurations were effectively reduced the turbulence intensity inside the cavity. By examining OASPL contours, it is seen that combined configurations have greatly reduced the OASPL near cavity front region compared to other methods.

OASPL distribution along the cavity floor at mid-plane is given in Figure 19 and it is obvious that the combined configurations have reduced the noise generation even further than PAW1 case which was the best method among all other configurations. Despite PAW1 is the best configuration in terms of OASPL reduction at cavity front wall and up to 20% of the cavity floor, PC2 case then reduces the noise significantly starting from 80% of the cavity floor including cavity aft wall. Isosurfaces of Q-criterion for combined configurations represent the rotational behavior of the flow when the attention is focused about the mid-section of the cavity in Figure 20. Counter rotating vortices are present as a result of both rotational nature of the flow and usage of spoilers ahead of the cavity. Less structures are also observed compared to M219CC configuration.

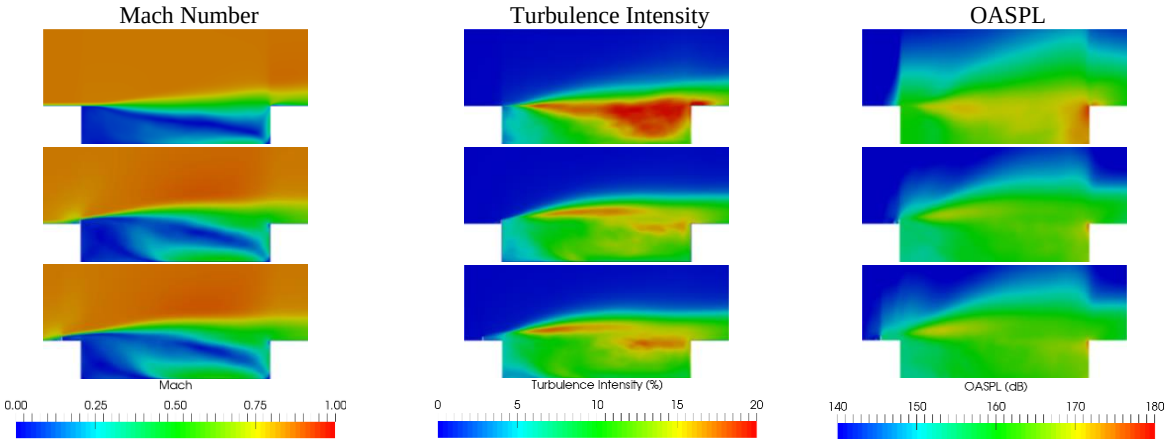

Figure 15. Mean Mach, turbulent intensity and OASPL (dB) contours for spoiler configurations a) M219CC b) PSP1 c) PSP2.

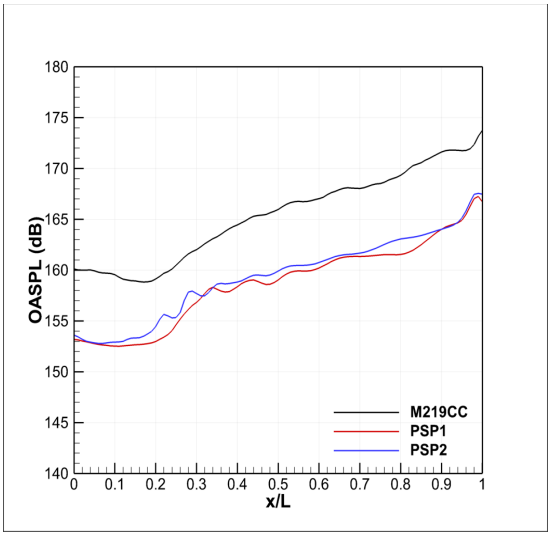

Figure 16. OASPL distribution at the mid-section of the cavity walls (front-floor-aft) for different spoiler configurations.

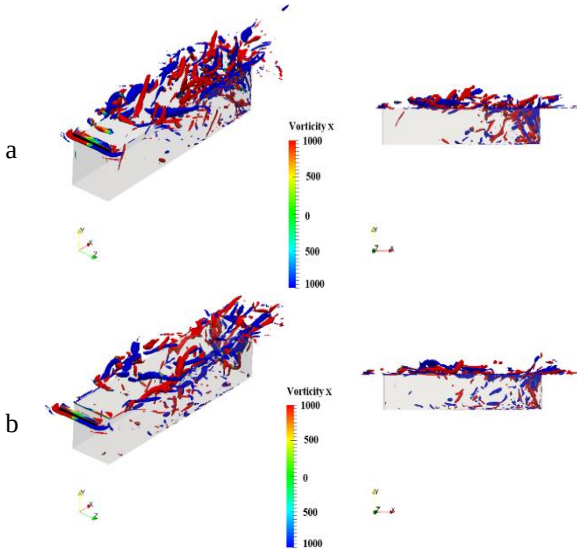

Figure 17. Isosurfaces of Q-criterion colored by Mach number for a) PSP1 b) PSP2, t=50 CTS (0.088s).

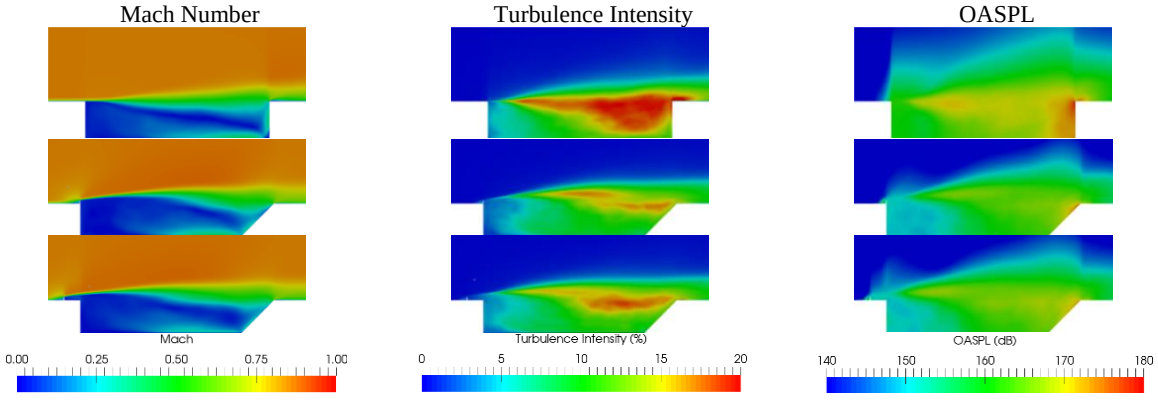

Figure 18. Mean Mach, turbulent intensity and OASPL (dB) contours for a) M219CC b) PC1 c) PC2.

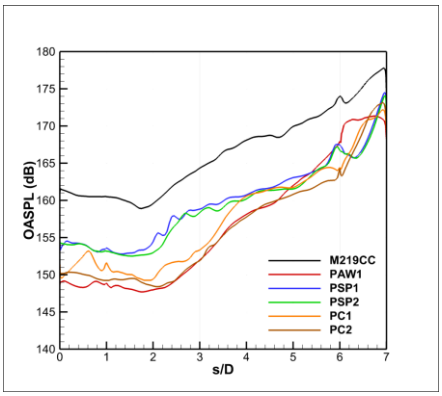

Figure 19. OASPL distribution at the mid-section of the cavity walls (front-floor-aft) for combined passive flow control configurations.

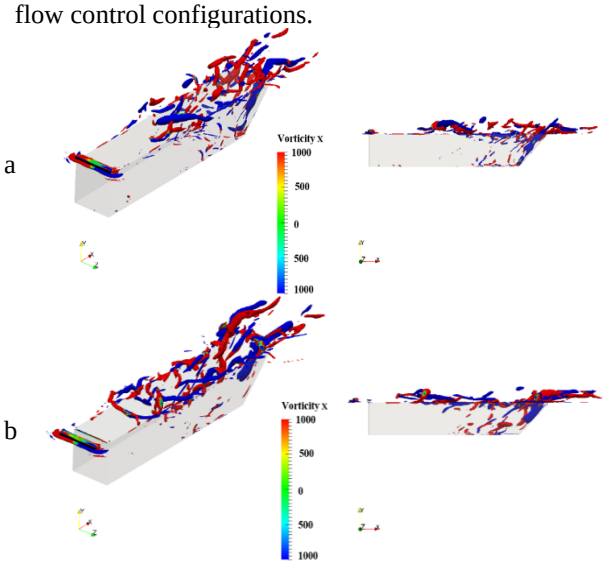

Figure 20. Isosurfaces of Q-criterion colored by Mach number for combined passive flow control configurations a) PC1 b) PC2, t=0.088 s.

3.6. Overall Comparison

Various passive flow control methods that are applied to the clean cavity configuration are compared with each other in terms of reduction of average OASPL generated along the cavity floor. This comparison is presented in Table 6. PAW1 configuration where aft wall of cavity is inclined with 45° has reduced the OASPL more than other aft wall configurations. The reduction was approximately 9.4 dB in magnitude and was around 5.7%. For spoiler configurations, both methods have similar influences on the OASPL. Lastly, PC2 configuration where PAW1 and PSP2 cases are combined and applied simultaneously, has reduced the average OASPL on cavity floor by 9.72 dB which corresponds to ~5.9%. Pressure fluctuations of a probe placed at 95% of the cavity floor for a selected configuration of each category are presented in Figure 21. In order to ease the visibility, the results are shown differently for each case. In Figure 21, fluctuations of pressure from 10 CTS to 40 CTS for M219CC and PAW1 configurations are compared. It is seen that severe fluctuations observed in M219CC are no longer present in PAW1 case. The level of fluctuations are reduced with the applied flow control method. Therefore, it can be implicated that the reduction in pressure fluctuations can also be a representative notation to noise reduction. Figure 21 shows that PC2 configuration were significantly attenuated the oscillatory behavior of pressure. Generally, each passive flow control method have successively suppressed the pressure oscillations compared to M219CC case.

Table 6. Average OASPL along the cavity floor for each configuration.

Configuration	AOASPL (dB)	Noise Reduction (dB)	Noise Reduction (%)
M219CC	164.88	--	--
PAW1	155.48	9.4	5.7011
PAW2	160.82	4.06	2.4624
PAW3	158.59	6.29	3.8149
PAW4	160.95	3.93	2.3836
PSP1	158.73	6.15	3.73
PSP2	159.35	5.53	3.354
PC1	156.21	8.67	5.2584
PC2	155.16	9.72	5.8952

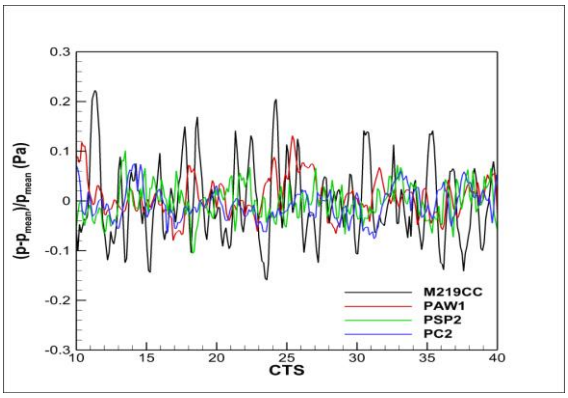

Figure 21. Comparison of pressure fluctuations at 0.95 x/L of cavity floor for passive flow control methods.

4. CONCLUSION

Numerical simulations of an open cavity with various novel passive flow control methods at a transonic speed where freestream Mach number was 0.85 were performed throughout this study. These novel passive flow control techniques were applied with the aim of reducing OASPL and suppressing severe pressure oscillations. Analyses were conducted via pressure-based transient flow solver rhoPimpleFoam of OpenFOAM® with $k-\omega SSTDES$ turbulence model.

The influence of y^+ on such an analysis was proven to be small since the flow is governed by large-scale coherent structures. To deduce an outcome from this, it may be stated that unsteady analyses of transonic cavity

flows might be accelerated without compromising from CFL number. M219CC analyses have shown that the flow is highly transient and unsteady which were not possible to examine using URANS methods. Due to this problem, DES methodology is followed.

PAW1 configuration decreased the average OASPL about ~9 dB. Large turbulent structures occurs on M219CC were also vanished in PAW1 configuration. PAW3 configuration which is potentially one of the main intriguing and original cases in the present study where the aft wall is reshaped in a stair-stepped manner, was also successful in terms of OASPL reduction, about ~6.29 dB. Turbulent coherent structures that are obviously seen everywhere in the cavity field in M219CC are also started to scatter and diminish in PAW3 case. Similar to PAW3, PAW4 configuration where spline shaped cavity aft wall is used, has decreased the generated noise by approximately 3.93 dB in overall. PAW3 case was also effective in terms of diminishing turbulent and chaotic flow field structure of M219CC. Spoilers were placed upstream wall of the cavity on the purpose of lifting or scattering the incoming boundary layer. These methods were successfully reduced the OASPL up to 7.5 dB. Lastly, combined configurations where spoiler and aft wall flow controls were applied simultaneously were investigated. These combined methods where advantages of both distinct flow control techniques are applied simultaneously contribute to the novelty of the present study along with the stair-stepped and spline shaped cavity aft wall configurations. Obtained results proved that the large-scale coherent structures were diminished since the flow were stabilized much more than the clean cavity configuration. Oscillations of pressure were also faded in parallel with this stabilization. All simulations presented in this study were run in parallel using 224 processors.

To the best of knowledge of this study's authors, nearly half of the passive flow control methods that were applied in the study such as combined spoiler and aft wall inclination, stair-stepped cavity aft wall or spline shaped cavity aft wall may have a potential to contribute to the development of passive flow control literature of cavity flows.

5. ACKNOWLEDGEMENTS

Studies within the scope of thesis were run on the National Center for High Speed Computing UHeM (http:(//en.uhem.itu.edu.tr/). This study is supported by the Turkish Aerospace Industries (https://tai.com.tr/en) under the grant of TM-2013. The author(s) are grateful to the authorized staff for their support, funding and assistance with this study.

6. REFERENCES

[1] K. Krishnamurty, "Acoustic radiation from two-dimensional rectangular cutouts in aerodynamics surfaces," NACA, California Institute of Technology, USA, Tech. Rep. 3487, 1955.

[2] A. Roshko, "Some Measurements of Flow in a Rectangular Cut-Out," NACA, California Institute of Technology, Tech. Rep. 3488, 1955.

[3] J. E. Rossiter, "A Preliminary Investigation into Armament Bay Buffet at Subsonic and Transonic Speeds," Royal Aircraft Establishment, Farnborough, UK, Technical Memorandum 679, 1960.

[4] S. H. Shih, A. Hamed, and J. Yeuan, "Unsteady supersonic cavity flow simulations using coupled k-epsilon and Navier-Stokes equations," AIAA Journal, vol. 32, no. 10, pp. 2015-2021, October 1994.

[5] R. L. Stallings Jr, and F. J. Wilcox Jr, "Experimental cavity pressure distributions at supersonic speeds," Scientif. and Techn. Information Branch, NASA, Washington, DC, NASA-TP-2683. 1987.

[6] E. B. Plentovich, R. L. Stallings, and M. B. Tracy, "Experimental cavity pressure measurements at subsonic and transonic speeds: Static-pressure results," Office of Management, Scientific and Technical Information Program, NASA, Washington, DC, NASA-TP-3358. 1993.

[7] S. Izawa, "Active and Passive Control of Flow Past a Cavity," *in Wind Tunnels and Experimental Fluid Dynamics Research*, J.C. Lerner, Ed. INTECH Open Access Publisher, 2011, pp. 369-394.

[8] D. A. Norton, "Investigation of B47 bomb bay buffet, " Boeing Airplane Co., USA, Doc. No. D12675, 1952.

[9] J. E. Rossiter, J. E, "Wind-tunnel experiments on the flow over rectangular cavities at subsonic and transonic speeds," Royal Aircraft Establishment London: H.M.S.O, UK, Tech. Rep. 64037, 1964.

[10] J.E. Rossiter, J. E. "The Effect of Cavities on the Buffeting of Aircraft," Royal Aircraft Establishment, Farnborough, UK, Technical Memorandum 754, 1962.

[11] A. M. Lamp, and N. Chokani, "Computation of Cavity Flows with Suppression Using Jet Blowing," *Journal of Aircraft*, vol. 34, no.4, pp. 545-551, July 1997.

[12] S. Arunajatesan, C. Kannepalli, N. Sinha, M. Sheehan, and G. Shumway, "Suppression of Cavity Loads Using Leading Edge Blowing Concepts," *46th AIAA Aerospace Sciences Meeting and Exhibit*, Reno, Nevada, 2008.

[13] S. J. Lawson and G. N. Barakos "Assessment of Passive Flow Control for Transonic Cavity Flow Using Detached-Eddy Simulation," *Journal of Aircraft*, vol. 46, no.3, pp. 1009-1029, May 2009.

[14] S. Lawson and G. Barakos, "Review of numerical simulations for high-speed, turbulent cavity flows," *Progress in Aerospace Sciences*, vol. 47, no.3, pp. 186-216, April 2011.

[15] L. N. Cattafesta, Q. Song, D. R. Williams, C. W. Rowley, and F. S. Alvi, "Active control of flow-

induced cavity oscillations," *Progress in Aerospace Sciences*, vol. 44, pp. 479-502, October 2008.

[16] L. Cattafesta, F. Alvi, D. Williams and C. Rowley, "Review of Active Control of Flow-Induced Cavity Oscillations (Invited)", in *33rd AIAA Fluid Dynamics Conference and Exhibit, Orlando, Florida, USA, June 23-26, 2003*.

[17] L. Shaw, R. Clark, and D. Talmadge, "F-111 generic weapons bay acoustic environment," *Journal of Aircraft*, vol. 25, no.2, pp. 147-153, February 1988.

[18] B. Smith, T. Welterlen, B. Maines, L. Shaw, M. Stanek and J. Grove, "Weapons bay acoustic suppression from rod spoilers," *40th AIAA Aerospace Sciences Meeting & Exhibit, Reno, NV, U.S.A, January 14-17, 2002*.

[19] A. J. Saddington, V. Thangamani, and K. Knowles, "Comparison of Passive Flow Control Methods for a Cavity in Transonic Flow," *Journal of Aircraft*, vol. 53, no.5, pp. 1439-1447, September 2016.

[20] A. F. Charwat, J. N. Roos, F. C. Dewey and J. A. Hitz, "An Investigation of Separated Flows - Part I: The Pressure Field," *Journal of the Aerospace Sciences*, vol. 28, no.6, pp. 457-470, June 1961.

[21] J. E. Rossiter and A. G. Kurn, "Wind Tunnel Measurements of the Unsteady Pressures in and behind a Bomb Bay," Royal Aircraft Establishment, Farnborough, UK, Technical Note 2845, 1962.

[22] O. Baysal, G. Yen and K. Fouladi, "Navier-Stokes Computations of Cavity Aeroacoustics with Suppression Devices," *Journal of Vibration and Acoustics*, vol. 116, pp. 105-112, January 1994.

[23] R. L. Sarno and M. E. Franke, "Suppression of flow-induced pressure oscillations in cavities," *Journal of Aircraft*, vol. 31, pp. 90-96, January 1994.

[24] R. L. Stallings Jr, E. B. Plentovich, M. B. Tracy and M. J. Hemsch, "Effect of Passive Venting on Static Pressure Distributions in Cavities at Subsonic and Transonic Speeds," NASA, USA, Technical Memorandum 4549, 1994.

[25] J. A. Ross and J. W. Peto, "Internal Stores Carriage Research at RAE," QinetiQ, UK, Technical Memorandum 2223, 1992.

[26] X. Zhang, and J. A. Edwards, "Pressure over a dual-cavity cascade at supersonic speeds," *The Aeronautical Journal*, vol. 103, pp. 45-54, January 1999.

[27] S. Arunajatesan, J. Shipman and N. Sinha, "Hybrid RANS-LES simulation of cavity flow fields with control," *40th AIAA Aerospace Sciences Meeting & Exhibit, Reno, NV, U.S.A., January 14-17, 2002*.

[28] L. S. Ukeiley, M. K. Ponton, J. M. Seiner and B. Jansen, "Suppression of Pressure Loads in Cavity Flows," *AIAA Journal*, vol. 42, pp. 70-79, January 2004.

[29] P. Nayyar, *CFD Analysis of Transonic Turbulent Cavity Flows.* PhD [Dissertation]. Glasgow, WA: Glasgow Univ., 2005, [Online]. Available: http://theses.gla.ac.uk/.

[30] P. Comte, F. Daude and I. Mary, "Simulation of the reduction of unsteadiness in a passively controlled transonic cavity flow," *Journal of Fluids and Structures*, vol. 24, pp. 1252-1261, November 2008.

[31] R. Ashworth, "DES of a Cavity with Spoiler," In *Advances* in *Hybrid RANS-LES Modelling* S.H. Peng, W. Haase, Ed. Springer, Berlin, Heidelberg, 2008, pp. 162-171.

[32] A. Omer, *Passive Methods for Suppressing Acoustic Resonance Excitation in Shallow Rectangular Cavities*. MSc [Dissertation]. Oshawa. WA: Ontario Institute of Technology Univ., 2014. [Online]. Available: http://ir.library.dc-uoit.ca/.

[33] Y. Wang, S. Li, and X. Yang, "Numerical investigation of the passive control of cavity flow oscillations by a dimpled non-smooth surface," *Applied Acoustics*, vol. 111, pp. 16-24, October 2016.

[34] C. J. Greenshields, "OpenFOAM user guide," *OpenFOAM Foundation Ltd, version 3*, 2015.

[35] D. P. Rizzetta and M. R. Visbal "Large-Eddy Simulation of Supersonic Cavity Flowfields Including Flow Control," *AIAA Journal*, vol. 41, pp. 1452-1462, August 2003.

[36] F. R. Menter, M. Kuntz and R. Langtry, "Ten years of industrial experience with the SST turbulence model," *Turbulence, Heat and Mass Transfer*, vol. 4, pp. 625-632, January 2003.

[37] L. Larchevêque, P. Sagaut, T. Lê, and P. Comte, "Large-eddy simulation of a compressible flow in a three-dimensional open cavity at high Reynolds number," *Journal of Fluid Mechanics*, vol. 516, pp. 265-301, September 2004.

[38] K. M. Guleren, S. Turk, O. M. Demircan and O. Demir, "Numerical Analysis of the Cavity Flow subjected to Passive Controls Techniques," in *3rd International Conference on Mechanical and Aeronautical Engineering, ICMAE 2017 Dubai, UAE, December 13-16, 2017*, pp. 012-015.

[39] H. K. Versteeg and W. Malalasekera, *An introduction to computational fluid dynamics: The finite volume method*. Harlow: Pearson Education, 2011.

[40] P. G. F. E. Freitas, *Numerical simulation of compressible flow over a deep cavity*, MSc [Dissertation]. Lisbon, WA: Superior Technical İnstitute 2014. [Online]. Available: http://fenix.tecnico.ulisboa.pt/.

[41] S. Das and J. Cohen, "Effect of rear face geometry on the open cavity oscillatory flow at M= 0.9," In *8th AIAA Flow Control Conference, Washington, D.C.,*

USA, June 13-17, 2016, pp. 3175.

[42] T. Gautam, G. Lovejeet and A. Vaidyanathan, "Experimental study of supersonic flow over cavity with aft wall offset and cavity floor injection," *Aerospace Science and Technology*, vol. 70, pp. 211-232, November 2017.

[43] K. Luo, W. Zhe, Z. Xiao and S. Fu, "Improved delayed detached-eddy simulations of sawtooth spoiler control before supersonic cavity," *International Journal of Heat and Fluid Flow*, vol. 63, pp. 172-189, February 2017.

[44] S. Mancini, A. Kolb, I. Gonzalez-Martino and D. Casalino, "Effects of wall modifications on pressure oscillations in high-subsonic and supersonic flows over rectangular cavities," In *25th AIAA/CEAS aeroacoustics conference Delft, The Netherlands, May 20-23, 2019*, pp. 2692.

[45] ESDU, *Aerodynamics and Aero-Acoustics of Rectangular Planform Cavities. Part I: Time-Averaged Flow*, 2004.

[46] D. Nightingale, J. A. Ross, and G. Foster, "Cavity Unsteady Pressure Measurements-Examples from Wind-Tunnel Tests," QinetiQ, Technical Report, 2005.

[47] T. V. Krishna, P. Kumar, S. Das, S. L. N. Desikan, "Effect of Cavity Rear Wall Modifications on Pressure Fluctuations at Supersonic Speeds," *Acta Astronautica*, vol. 185, pp. 78-88, May 2021.

VITAE

Oğuzhan DEMİR received his B.Sc. degree in Aeronautical Engineering from Faculty of Aeronautics and Astronautics, University of Turkish Aeronautical Association, Turkey in 2016. He received his M.Sc. degree in Aeronautical Engineering from Faculty of Aeronautics and Astronautics, Istanbul Technical University, Turkey in 2019. He is currently working at Roketsan Missiles Inc. Company as Aerodynamics Engineer.

Bayram ÇELİK received his B.Sc. degree in Astronautical Engineering from Faculty of Aeronautical and Astronautical Engineering, Istanbul Technical University, Turkey in 1993. He received his M.Sc. and Ph.D. degrees in Aeronautical and Astronautical Engineering from Istanbul Technical University, Turkey in 1997 and 2006, respectively. He is currently working at Istanbul Technical University as Associate Professor.

Kürşad Melih GÜLEREN received his B.Sc. degree in Aerospace Engineering from Faculty of Engineering, Middle East Technical University, Turkey in 1999. He received his M.Sc. degree in Mechanical Engineering from Cumhuriyet University, Turkey in 2003. He received his Ph.D. degree in Mechanical Engineering from The University of Manchester, England in 2007. He is currently working at Eskisehir Technical University as Professor.